

## FREE VIBRATION OF THERMALLY PRE/POST-BUCKLED CIRCULAR THIN PLATES EMBEDDED WITH SHAPE MEMORY ALLOY FIBERS

Shi-Rong Li<sup>1,2</sup>, Wen-Shan Yu<sup>2</sup>, and R. C. Batra<sup>3</sup>

<sup>1</sup>School of Civil Science and Engineering, Yangzhou University, Yangzhou, Jiangsu, China

<sup>2</sup>Department of Engineering Mechanics, Lanzhou University of Technology, Lanzhou, Gansu, China

<sup>3</sup>Department of Engineering Science and Mechanics, Virginia Polytechnic Institute and State University, Blacksburg, VA, USA

*Axisymmetric deformations of a uniformly heated pre-buckled and post-buckled thin circular plate reinforced with shape memory alloy (SMA) fibers placed in the radial direction only are studied. Effects of von Kármán's nonlinearities are incorporated in the problem formulation. The matrix is assumed to be linear thermoelastic and the thermo-mechanical response of the SMA is modeled by one-dimensional constitutive relation. By assuming that plate's deflections can be additively decomposed into three parts, namely radial displacements of a pre-buckled plate, radial and lateral displacements during post-buckling deformations, and infinitesimal radial and lateral displacements during vibration of a post-buckled plate, boundary-value problems for determining these displacements for plate edges either simply supported or clamped have been formulated. The coupled nonlinear differential equations have been numerically solved by the shooting method that has been verified by good agreement between the presently computed results with those available in the literature. The dependence of the first three frequencies upon the temperature rise, for both pre-buckled and post-buckled plates, has been delineated. Characteristic curves relating the frequency with the temperature rise for different values of the volume fraction and the pre-strain in the SMA fibers are exhibited. It is found that reinforcement of an aluminum plate with SMA fibers changes plate's natural frequencies and enhances its resistance to buckling due to temperature rise.*

**Keywords:** Circular plate; Natural frequencies; Pre-buckling and post-buckling; Shape memory alloy; Shooting method

Received 8 January 2009; accepted 16 May 2009.

SRLs and WSYs work was supported by the National Natural Science Foundation of China grant numbers 10872083 and 10602021, and the Fund of the Ministry of Education of China for Supervisors of Doctorate Students (200807310002). RCB's work was partially funded by the U.S. Office of Naval Research grants N00014-06-1-0567 and N00014-06-1-0913 to Virginia Polytechnic Institute and State University. The authors gratefully acknowledge these financial supports. Views expressed in the paper are those of authors and neither of the funding agencies nor of their institutions.

Address correspondence to Shi-Rong Li, School of Civil Science and Engineering, Yangzhou University, Yangzhou, Jiangsu 225009, China. E-mail: list2000@yahoo.com.cn

## INTRODUCTION

Plates are key components in many structural applications. Buckling and vibration of plates due to thermal loads play important roles in the design and analysis of aerospace, off-shore, under-water, nuclear, and electronic components/structures. Static and dynamic responses of plates and shells exposed to thermal environments have been reviewed by Tauchert [1] and Thorton [2]. Even though there have been extensive investigations on the thermal buckling of plates, the dynamic response of post-buckled circular plates has not been studied thoroughly. The vibration response of flat and curved panels subjected to thermo-mechanical loads has been studied by Librescu et al. [3, 4]. Li and Zhou [5, 6] used the shooting method to analyze vibrations of uniformly heated orthotropic circular/annular plates. Lee and Lee [7] examined vibrations of pre-buckled and post-buckled anisotropic plates by using the first-order shear deformation plate theory (FSDT). Free vibration response of a thermally buckled piezo-laminated composite plate has been investigated by Oh et al. [8] by using the finite element method (FEM). Infinitesimal vibrations of a post-buckled functionally graded plate have been studied by Park and Kim [9], and of a statically deformed pre-buckled or post-buckled plate by Li and Batra [10].

Studies [3–10] on vibration of heated thin plates and shells reveal that natural frequencies of a thermally loaded structure are noticeably affected by the temperature rise. However, effects of temperature rise on free vibration of plates embedded with shape memory alloy (SMA) fibers will be more significant because the temperature rise will change the pre-strain in the fiber and may induce a phase transformation in the SMA fibers that will alter their mechanical properties. Many research efforts have contributed to our understanding of the vibration and the buckling control of plates reinforced with SMA fibers. Rogers et al. [11–13] experimentally and analytically investigated the acoustic and vibration control of an SMA hybrid composite plate made of graphite/epoxy and NiTiNol/epoxy laminas. Ro and Baz [14] studied effects of activating NiTiNol fibers on the buckling and vibration of SMA reinforced composite plate by the FEM coupled with experimental observations. Ostachowicz et al. [15, 16] used the FEM to examine in detail effects of embedding SMA actuators on the natural frequencies and thermal buckling of laminated plates. Based on the FSDT, thermal buckling and linear vibration of pre-buckled and post-buckled SMA fiber-reinforced laminated composite plates were examined by Zhong et al. [17, 18] and Park et al. [19, 20]. They used the FEM to analyze the influence of the volume fraction and the initial strain of SMA fibers on natural frequencies and buckling deflection of plates. It should be noted that they used experimental data to model the recovery stress and Young's modulus versus the temperature rise instead of an analytical constitutive relation for the SMA, and found that the SMA fibers could greatly reduce or completely eliminate the post-buckling deflection for appropriate values of the temperature rise.

Lee et al. [21] used the commercial FE computer code ABAQUS to analyze laminated composites shells and plates with embedded SMA wires, and showed that the activation of SMA wires due to heating increases the critical buckling temperature and decreases the thermal buckling deformation. Thompson and Loughlan's extensive experimental and numerical simulations [22, 23] indicate that

recovery forces in pre-strained SMA fibers produced by thermal activation enhance the buckling temperature for various laminated plates and reduce the out-of-plane displacement of the post-buckled laminates. More recently, Zhang et al. [24] studied vibration of laminated composite plates with embedded SMAs by using the Rayleigh-Ritz method. In the aforementioned investigations, the SMA fiber-reinforced composite structures are either beams or rectangular plates.

We study here thermally induced pre-buckling and post-buckling deformations of a circular plate reinforced with SMA fibers. We use the one-dimensional constitutive relation proposed by Brinson [25] to find the recovery stress in the SMA fiber. The plate edge is either simply supported with boundary points restrained from moving in the radial direction or clamped. The strain-displacement relations incorporate von Kármán nonlinearities and the stress-strain relation is taken to be linear. The nonlinear governing equations are numerically solved with the shooting method to analyze the pre-buckling and the post-buckling deformations of the plate. Numerical results presented herein include the thermal post-buckled equilibrium paths and frequencies of free vibrations of post-buckled configurations.

## PROBLEM FORMULATION

We consider a thin composite circular plate of radius  $b$  and thickness  $h$  composed of an isotropic and homogenous matrix, and reinforced shape memory alloy (SMA) fibers in the radial direction. A cylindrical co-ordinate system  $(r, \theta, z)$  located in the mid-surface of the plate as shown in Figure 1 is used to describe plate's deformations. The material of plate is considered to be polar orthotropic. We assume that a steady uniform temperature change  $T$  is applied to the plate, and the plate particles at its boundary are restrained from moving within the mid-surface so that in-plane thermal stresses are induced due to the temperature change. We study axisymmetric free vibration of the pre-buckled and the post-buckled heated plate by incorporating the von Kármán nonlinearity in the Kirchhoff plate theory. The strain-displacement relations are

$$\varepsilon_r = \frac{\partial u}{\partial r} + \frac{1}{2} \left( \frac{\partial w}{\partial r} \right)^2 - z \frac{\partial^2 w}{\partial r^2} \quad \varepsilon_\theta = \frac{u}{r} - \frac{z}{r} \frac{\partial w}{\partial r}, \quad \gamma_{r\theta} = \gamma_{\theta r} = 0 \quad (1)$$

where  $u(r, t)$ ,  $w(r, t)$  are the radial and the transverse displacements of a point on the mid-surface;  $t$  the time;  $\varepsilon_r$  and  $\varepsilon_\theta$  the radial and the circumferential strains, respectively;  $\gamma_{r\theta}$  the shear strain.

We assume that the material response for infinitesimal deformations of the elastic composite plate can be adequately described by the following constitutive equations [17–20]:

$$\sigma_r = \frac{E_r}{1 - \mu_{r\theta}\mu_{\theta r}} [\varepsilon_r + \varepsilon_\theta \mu_{\theta r} - (\alpha_r + \alpha_\theta \mu_{\theta r}) \Delta T] + \sigma_s V_s \quad (2)$$

$$\sigma_\theta = \frac{E_\theta}{1 - \mu_{r\theta}\mu_{\theta r}} [\varepsilon_\theta + \varepsilon_r \mu_{r\theta} - (\alpha_\theta + \alpha_r \mu_{r\theta}) \Delta T] \quad (3)$$

In Eqs. (2) and (3),  $E_r$  and  $E_\theta$  are Young's moduli in the radial and the circumferential directions, respectively;  $\alpha_r$  and  $\alpha_\theta$  the thermal expansion coefficients;

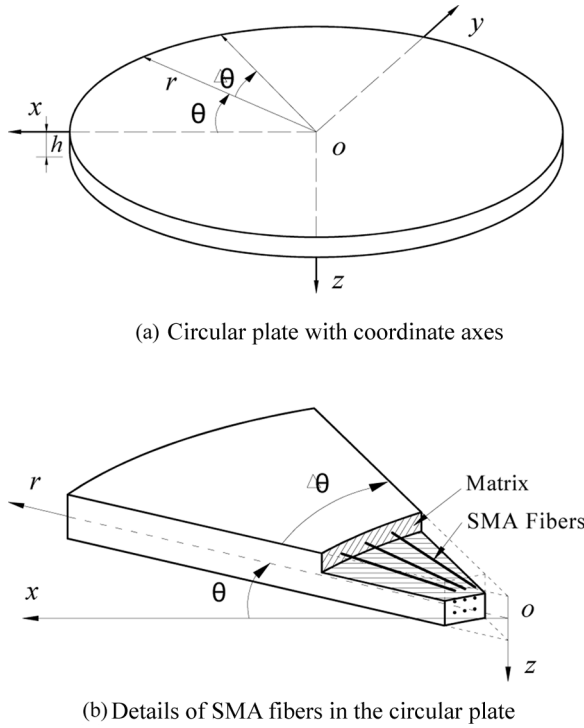


**Figure 1** Schematic sketch of the circular plate with SMA fibers embedded in the radial direction.

$\mu_{r\theta}$  and  $\mu_{\theta r}$  Poisson's ratios;  $\Delta T = T - T_0$  the temperature rise;  $T_0$  the initial temperature;  $\sigma_r$  and  $\sigma_\theta$  normal stresses in the radial and the circumferential directions;  $\sigma_s$  the recovery stress induced by the inverse martensitic transformation of the SMA due to the temperature change  $\Delta T$ ;  $V_s$  the volume fraction of the SMA fibers taken to be uniform in the plate. The assumptions of  $V_s$  being constant and the stress in the SMA affecting only  $\sigma_r$  greatly simplify the problem. If SMA reinforcements are wires then for  $V_s$  to be constant either their diameter will need to decrease with the radial coordinate or the spacing between two adjacent wires will have to increase. In Eqs. (2) and (3) we have assumed that  $E_z = E_r$ .

Homogenization techniques for deriving effective properties of composites with SMA as reinforcements have been discussed, for example, in [31–35]. Effective values of material parameters in terms of those of the matrix and the SMA given in Appendix A are derived by the mechanics of materials approach.

Using one-dimensional constitutive equations for SMA, the recovery stress of SMA fibers is given by the following relation [21, 25]:

$$\sigma_s = [E(\xi) - E(\xi_0)]\varepsilon_0 + \Omega(\xi)\xi_s - \Omega(\xi_0)\xi_{s0} + \Theta(T - T_0) \quad (4a)$$

$$E(\xi) = E_A + \xi(E_M - E_A), \quad \Omega(\xi) = -\varepsilon_L E(\xi) \quad (4b)$$

where  $E(\xi)$ ,  $\Omega(\xi)$ ,  $\Theta$ ,  $\xi$ ,  $\varepsilon_0$  and  $\varepsilon_L$  are, respectively, Young's modulus, the phase transformation coefficient, the coefficient of thermal expansion, the volume fraction of martensite, the initial axial strain, and the maximum residual strain of SMA fibers. Quantities with the subscript "0" denote their values in the initial state of SMA.  $E_M$  and  $E_A$  are, respectively, Young's moduli of the SMA in the pure martensite and the pure austenite phases. The parameter  $\xi$  defined in the range  $[0, 1]$  is divided into the stress-induced part  $\xi_s$  and the temperature-induced part  $\xi_T$ . Here we only consider temperature rise.

For  $T > A_s$  and  $C_A(T - A_f) < \sigma_s < C_A(T - A_s)$ ,  $\xi$ ,  $\xi_s$  and  $\xi_T$  are computed from the following relations [25]:

$$\xi = \frac{\xi_0}{2} \left\{ \cos \left[ a_A \left( T - A_s - \frac{\sigma_s}{C_A} \right) \right] + 1 \right\} \quad (4c)$$

$$\xi_s = \xi_{s0} - \frac{\xi_{s0}}{\xi_0} (\xi_0 - \xi) \quad (4d)$$

$$\xi_T = \xi_{T0} - \frac{\xi_{T0}}{\xi_0} (\xi_0 - \xi) \quad (4e)$$

where  $A_s$  and  $A_f$  denote the austenite transformation start and finish temperature respectively,  $C_A$  equals the slope of the curve of the critical stress for austenite phase transformation as function of temperature,  $a_A = \pi/(A_f - A_s)$ , and  $\xi_{T0}$  is the initial volume fraction of martensite.

Substitution from Eq. (1) into Eqs. (2) and (3), and integrating their zeroth order and first order moments with respect to the thickness coordinate  $z$  over the plate thickness give following expressions for the membrane forces and the bending moments:

$$N_r = \int_{-h/2}^{h/2} \sigma_r dz = C \left[ \frac{\partial u}{\partial r} + \frac{1}{2} \left( \frac{\partial w}{\partial r} \right)^2 + \frac{\mu_{\theta r}}{r} u - \alpha_r (1 + \beta \mu_{\theta r}) \Delta T \right] + \sigma_s V_s h \quad (5a)$$

$$N_\theta = \int_{-h/2}^{h/2} \sigma_\theta dz = C \left[ \mu_{\theta r} \left( \frac{\partial u}{\partial r} + \frac{1}{2} \left( \frac{\partial w}{\partial r} \right)^2 \right) + \frac{k}{r} u - \alpha_r (k\beta + \mu_{\theta r}) \Delta T \right] \quad (5b)$$

$$M_r = \int_{-h/2}^{h/2} \sigma_{rz} dz = -D \left( \frac{\partial^2 w}{\partial r^2} + \frac{\mu_{\theta r}}{r} \frac{\partial w}{\partial r} \right) \quad (6a)$$

$$M_\theta = \int_{-h/2}^{h/2} \sigma_\theta z dz = -D \left( \mu_{\theta r} \frac{\partial^2 w}{\partial r^2} + \frac{k}{r} \frac{\partial w}{\partial r} \right) \quad (6b)$$

where  $k = E_\theta/E_r = \mu_{\theta r}/\mu_{r\theta}$  is the ratio of elastic moduli,  $\beta = \alpha_\theta/\alpha_r$  is the ratio of coefficients of thermal expansion,  $C = 12D/h^2$  and  $D = E_r h^3/[12(1 - \mu_{\theta r}\mu_{r\theta})]$  are the in-plane and the flexural rigidities of the plate.

We introduce the following non-dimensional quantities.

$$(x, U, W) = (r, u, w)/b, \quad \delta = b/h \quad (7a)$$

$$\lambda = 12\delta^2(1 + \mu_{\theta r}\beta)\alpha_r\Delta T, \quad s = (\mu_{\theta r} + \beta k)/(1 + \beta\mu_{\theta r}) \quad (7b)$$

$$N^* = \sigma_s V_s (1 - \mu_{\theta r}\mu_{r\theta})/E_r, \quad \tau = (t/b^2)(D_r/\rho h)^{1/2} \quad (7c)$$

where  $\rho$ , defined in Appendix A, is the mass density of the homogenized plate.

By neglecting the in-plane and the rotary inertia and using Hamilton's principle, we obtain the following partial differential equations and the associated boundary conditions governing free vibration of the circular plate in terms of non-dimensional variables [5, 6, 10].

$$\frac{\partial^2 U}{\partial x^2} + \frac{1}{x} \frac{\partial U}{\partial x} - \frac{k}{x^2} U + \frac{\partial W}{\partial x} \frac{\partial^2 W}{\partial x^2} + \frac{1 - \mu_{0r}}{2x} \left( \frac{\partial W}{\partial x} \right)^2 = \frac{1}{x} \left[ \frac{\lambda}{12\delta^2} (1 - s) - N^* \right] \quad (8)$$

$$\begin{aligned} & \frac{\partial^4 W}{\partial x^4} + \frac{2}{x} \frac{\partial^3 W}{\partial x^3} - \frac{k}{x^2} \frac{\partial^2 W}{\partial x^2} + \frac{k}{x^3} \frac{\partial W}{\partial x} + (\lambda - 12\delta^2 N^*) \left( \frac{\partial^2 W}{\partial x^2} + \frac{1}{x} \frac{\partial W}{\partial x} \right) + \frac{\partial^2 W}{\partial \tau^2} \\ & = 12\delta^2 \frac{1}{x} \frac{\partial}{\partial x} \left[ x \left( \frac{\partial U}{\partial x} + \frac{1}{2} \left( \frac{\partial W}{\partial x} \right)^2 + \frac{\mu_{0r}}{x} U \right) \frac{\partial W}{\partial x} \right] \end{aligned} \quad (9)$$

$$U = 0, \quad \frac{\partial W}{\partial x} = 0, \quad \frac{\partial^3 W}{\partial x^3} + \frac{1}{x} \frac{\partial^2 W}{\partial x^2} = 0, \quad \text{at } x = c \quad (10a,b,c)$$

$$U = 0, \quad W = 0, \quad \frac{\partial W}{\partial x} + K \frac{\partial^2 W}{\partial x^2} = 0, \quad \text{at } x = 1 \quad (11a,b,c)$$

The parameter  $c$  is a small positive real number introduced to avoid a singularity at  $x = 0$  while computing numerical results [5, 29], and  $K = 0$  and  $1/\mu_{0r}$ , respectively, for the clamped and the simply supported edges. Boundary conditions (10b) and (10c) imply that the transverse shear force  $Q_x = -\left(\frac{\partial^3 W}{\partial x^3} + \frac{1}{x} \frac{\partial^2 W}{\partial x^2} - \frac{1}{x^2} \frac{\partial W}{\partial x}\right)$  vanishes at  $x = c$ . In the limit of  $c$  approaching zero boundary conditions (10) are satisfied at the center of a solid circular plate.

## GOVERNING EQUATIONS FOR INCREMENTAL DISPLACEMENTS

In order to study infinitesimal vibration and static small deformations of the thermally buckled circular plate we assume that the solution of Eqs. (7)–(10) can be expressed as [3–6, 10]

$$U(x, \tau) = U_0(x) + U_s(x) + U_d(x, \tau) \quad (12)$$

$$W(x, \tau) = W_s(x) + W_d(x, \tau) \quad (13)$$

where  $U_0(x)$  is the in-plane radial displacement of the pre-buckled plate,  $U_s(x)$  and  $W_s(x)$  are the radial and the circumferential displacements of the thermally post-buckled plate,  $U_d(x, \tau)$  and  $W_d(x, \tau)$  are infinitesimal displacements superimposed on the thermally buckled configuration of the plate.

The displacement  $U_0$  is the solution of the boundary-value problem

$$\frac{d^2 U_0}{dx^2} + \frac{1}{x} \frac{dU_0}{dx} - \frac{k}{x^2} U_0 = \frac{1}{x} \left[ \frac{\lambda}{12\delta^2} (1 - s) - N^* \right] \quad (14)$$

$$U_0(c) = U_0(1) = 0 \quad (15)$$

whose analytical solution is [5, 6, 10]

$$U_0(x) = \begin{cases} \frac{B}{1-k} \left[ \frac{(c - c^{-\sqrt{k}})x^{\sqrt{k}} - (c - c^{\sqrt{k}})x^{-\sqrt{k}}}{c^{\sqrt{k}} - c^{-\sqrt{k}}} + x \right] & k \neq 1 \\ 0 & k = 1 \end{cases} \quad (16)$$

where  $B = [\lambda(1 - \varsigma)/12\delta^2 - N^*]$ . In the limit  $c \rightarrow 0$ , Eq. (16) gives [10]

$$U_0(x) = \begin{cases} \frac{B}{1-k} [x - x^{\sqrt{k}}] & k \neq 1 \\ 0 & k = 1 \end{cases} \quad (17)$$

For  $\varsigma = 1$  and  $N^* = 0$  Eq. (14) with boundary conditions given by Eq. (15) has a trivial solution  $U_0 = 0$ . For  $\varsigma \neq 1$  and  $N^* = 0$ , the problem reduces to that studied in [10]. Thus the present work differs from our earlier work [10] in  $N^*$  not being zero because of the stress induced in the SMA.

The incremental displacements,  $U_s(x)$  and  $W_s(x)$ , from the buckled to the post-buckled configurations are determined by solving the following non-linear boundary-value problem [10]:

$$\frac{d^2 U_s}{dx^2} + \frac{1}{x} \frac{dU_s}{dx} - \frac{k}{x^2} U_s + \frac{dW_s}{dx} \frac{d^2 W_s}{dx^2} + \frac{1 - \mu_{\theta r}}{2x} \left( \frac{dW_s}{dx} \right)^2 = 0 \quad (18)$$

$$\begin{aligned} & \frac{d^4 W_s}{dx^4} + \frac{2}{x} \frac{d^3 W_s}{dx^3} - \frac{k}{x^2} \frac{d^2 W_s}{dx^2} + \frac{k}{x^3} \frac{dW_s}{dx} + (\lambda - 12\delta^2 N^*) \left( \frac{d^2 W_s}{dx^2} + \frac{1}{x} \frac{dW_s}{dx} \right) \\ & = 12\delta^2 \frac{1}{x} \frac{d}{dx} \left[ x \left( \frac{dU_0}{dx} + \frac{dU_s}{dx} + \frac{1}{2} \left( \frac{dW_s}{dx} \right)^2 + \frac{\mu_{\theta r}}{x} (U_0 + U_s) \right) \frac{dW_s}{dx} \right] \end{aligned} \quad (19)$$

$$U_s = 0, \quad \frac{dW_s}{dx} = 0, \quad \frac{d^3 W_s}{dx^3} + \frac{1}{x} \frac{d^2 W_s}{dx^2} = 0, \quad \text{at } x = c \quad (20)$$

$$U_s = 0, \quad W_s = 0, \quad \frac{dW_s}{dx} + K \frac{d^2 W_s}{dx^2} = 0, \quad \text{at } x = 1 \quad (21)$$

Deformations of the SMA affect  $U_s(x)$  and  $W_s(x)$  through the presence of  $U_0$  in Eq. (19).

For studying infinitesimal vibration of the post-buckled plate, we neglect terms nonlinear in  $U_d(x, \tau)$  and  $W_d(x, \tau)$ . Substitution from Eqs. (12)–(13) into Eqs. (8)–(11), using Eqs. (18)–(21), we obtain the following linear homogeneous partial differential equations for finding  $U_d(x, \tau)$  and  $W_d(x, \tau)$ .

$$\frac{\partial^2 U_d}{\partial x^2} + \frac{1}{x} \frac{\partial U_d}{\partial x} - \frac{k}{x^2} U_d + \frac{dW_s}{dx} \frac{\partial^2 W_d}{\partial x^2} + \frac{\partial W_d}{\partial x} \frac{d^2 W_s}{dx^2} + \frac{1 - \mu_{\theta r}}{x} \frac{dW_s}{dx} \frac{\partial W_d}{\partial x} = 0 \quad (22)$$

$$\frac{\partial^4 W_d}{\partial x^4} + \frac{2}{x} \frac{\partial^3 W_d}{\partial x^3} - \frac{k}{x^2} \frac{\partial^2 W_d}{\partial x^2} + \frac{k}{x^3} \frac{\partial W_d}{\partial x} + (\lambda - 12\delta^2 N^*) \left( \frac{\partial^2 W_d}{\partial x^2} + \frac{1}{x} \frac{\partial W_d}{\partial x} \right) + \frac{\partial^2 W_d}{\partial \tau^2}$$

$$\begin{aligned}
&= 12\delta^2 \frac{1}{x} \frac{\partial}{\partial x} x \left[ \left( \frac{dU_0}{dx} + \frac{dU_s}{dx} + \frac{1}{2} \left( \frac{dW_s}{dx} \right)^2 + \frac{\mu_{0r}}{x} (U_0 + U_s) \right) \frac{\partial W_d}{\partial x} \right. \\
&\quad \left. + \left( \frac{\partial U_d}{\partial x} + \frac{dW_s}{dx} \frac{\partial W_d}{\partial x} + \frac{\mu_{0r}}{x} U_d \right) \frac{dW_s}{dx} \right] \quad (23)
\end{aligned}$$

$$U_d = 0, \quad \frac{\partial W_d}{\partial x} = 0, \quad \frac{\partial^3 W_d}{\partial x^3} + \frac{1}{x} \frac{\partial^2 W_d}{\partial x^2} = 0, \quad \text{at } x = c \quad (24)$$

$$U_d = 0, \quad W_d = 0, \quad \frac{\partial W_d}{\partial x} + K \frac{\partial^2 W_d}{\partial x^2} = 0, \quad \text{at } x = 1 \quad (25)$$

Thus deformations of SMAs influence  $U_d(x, \tau)$  and  $W_d(x, \tau)$  because  $U_0$  and  $N^*$  appear in Eq. (23).

We assume that Eqs. (22)–(25) have harmonic solutions [3–6, 10]

$$U_d(x, \tau) = \zeta(x) \cos(\omega\tau), \quad W_d(x, \tau) = \eta(x) \cos(\omega\tau) \quad (26)$$

where

$$\omega = \Omega \sqrt{\frac{\rho h b^4}{D_r}}$$

is the non-dimensional frequency and  $\Omega$  the dimensional frequency. Substitution from Eq. (26) into Eqs. (22)–(25) yields the following ordinary differential equations for amplitudes  $\zeta(x)$  and  $\eta(x)$ :

$$\frac{d^2 \zeta}{dx^2} + \frac{1}{x} \frac{d\zeta}{dx} - \frac{k}{x^2} \zeta + \frac{dW_s}{dx} \frac{d^2 \eta}{dx^2} + \frac{d\eta}{dx} \frac{d^2 W_s}{dx^2} + \frac{1 - \mu_{0r}}{x} \frac{dW_s}{dx} \frac{d\eta}{dx} = 0 \quad (27)$$

$$\begin{aligned}
&\frac{d^4 \eta}{dx^4} + \frac{2}{x} \frac{d^3 \eta}{dx^3} - \frac{k}{x^2} \frac{d^2 \eta}{dx^2} + \frac{k}{x^3} \frac{d\eta}{dx} + (\lambda - 12\delta^2 N^*) \left( \frac{d^2 \eta}{dx^2} + \frac{1}{x} \frac{d\eta}{dx} \right) - \omega^2 \eta \\
&= 12\delta^2 \frac{1}{x} \frac{d}{dx} x \left[ \left( \frac{dU_0}{dx} + \frac{dU_s}{dx} + \frac{1}{2} \left( \frac{dW_s}{dx} \right)^2 + \frac{\mu_{0r}}{x} (U_0 + U_s) \right) \frac{d\eta}{dx} \right. \\
&\quad \left. + \left( \frac{d\zeta}{dx} + \frac{dW_s}{dx} \frac{d\eta}{dx} + \frac{\mu_{0r}}{x} \zeta \right) \frac{dW_s}{dx} \right] \quad (28)
\end{aligned}$$

$$\zeta = 0, \quad \frac{d\eta}{dx} = 0, \quad \frac{d^3 \eta}{dx^3} + \frac{1}{x} \frac{d^2 \eta}{dx^2} = 0, \quad \text{at } x = c \quad (29)$$

$$\zeta = 0, \quad \eta = 0, \quad \frac{d\eta}{dx} + K \frac{d^2 \eta}{dx^2} = 0, \quad \text{at } x = 1 \quad (30)$$

We note that Eqs. (27)–(30) give amplitudes of free vibration of SMA fiber-reinforced composite plate with initial radial and lateral displacements  $U_0(x) + U_s(x)$  and  $W_s(x)$ , respectively. However, before solving Eqs. (27)–(30), we need first to solve the non-linear and coupled Eqs. (18)–(21) for  $U_s(x)$  and  $W_s(x)$ . If let  $U_s(x) = W_s(x) = 0$ , or the plate has not buckled, then Eqs. (27)–(30) can be reduced to governing equations for the linear vibration of the pre-buckled plate.

**Table 1** Material properties of the SMA fibers

$C_M = 8 \text{ MPa}/^\circ\text{C}$	$M_f = 9^\circ\text{C}$	$\Theta = 0.55 \text{ MPa}/^\circ\text{C}$	$\varepsilon_L = 0.067$
$C_A = 13.8 \text{ MPa}/^\circ\text{C}$	$M_s = 18.4^\circ\text{C}$	$\alpha_s = 10.26 \times 10^{-6}/^\circ\text{C}$	$\mu_s = 0.33$
$\sigma_s^{cr} = 100 \text{ MPa}$	$A_s = 34.5^\circ\text{C}$	$\rho_s = 6500 \text{ kg}/\text{m}^3$	$E_M = 26.3 \times 10^3 \text{ MPa}$
$\sigma_f^{cr} = 170 \text{ MPa}$	$A_f = 49^\circ\text{C}$		$E_A = 67 \times 10^3 \text{ MPa}$

## NUMERICAL RESULTS AND DISCUSSION

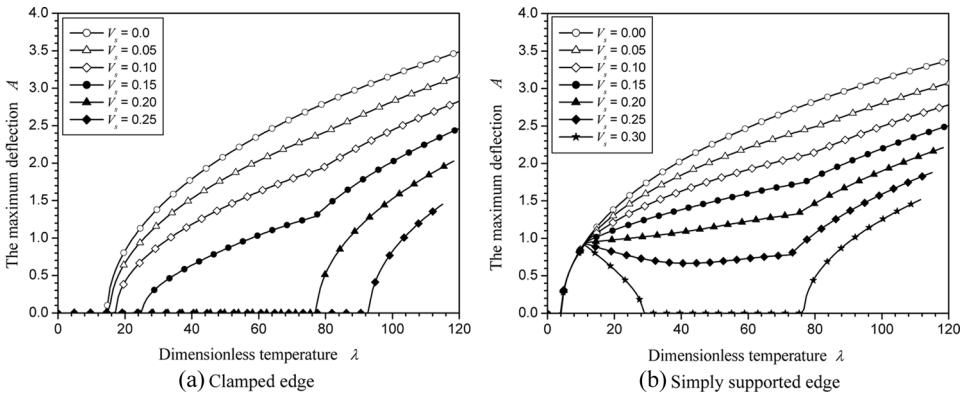
Because of our inability to analytically solve the nonlinear boundary-value problem defined by Eqs. (18)–(21) we solve it numerically with the shooting method that replaces the two-point boundary-value problem by a sequence of initial-value problems. As described in [5, 6, 10, 26], values of functions at the initial point,  $x = c$ , are estimated to start the computations. These are iterated upon with modified values obtained by the secant method until the prescribed boundary conditions at the final point  $x = 1$  are satisfied. It should be noted that the constitutive Eq. (4) is nonlinear and an explicit form for the recovery stress cannot be obtained; it is determined by the Newton–Raphson method.

While solving the problem numerically, we set initial temperature  $T_0 = 20^\circ\text{C}$ ,  $\delta = b/h = 30$ , and take  $c = 0.001$ . The matrix of the composite plate is aluminum for which  $\rho_m = 2800 \text{ kg}/\text{m}^3$ ,  $E_m = 70 \text{ GPa}$ ,  $\mu_m = 0.3$ ,  $\alpha_m = 23.4 \times 10^{-6}/^\circ\text{C}$ , and material properties the NiTiNi SMA, taken from [25], are listed in Table 1.

The numerical algorithm has been verified by comparing computed results for a few problems with those available in the literature; e.g., see Tables 1–3 of [10]. Results presented emphasize effects of the initial pre-strain and the volume fraction  $V_s$  of SMA fibers on the pre- and the post-buckling deformations of the plate.

### Thermal Buckling

The post-buckling equilibrium paths, in terms of the maximum deflection  $A = W(0)$  and the thermal load  $\lambda$ , of clamped and simply supported plates for known values of the SMA volume fraction,  $V_s$ , are plotted in Figure 2 with  $\varepsilon_0 = 0.04$  as

**Figure 2** Equilibrium paths of post-buckled circular plate for specified values of  $V_s$  ( $\varepsilon_0 = 0.04$ ).

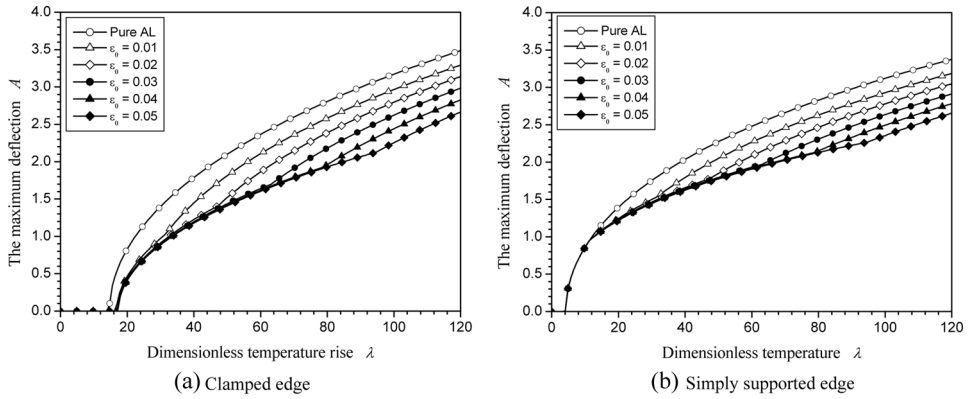


**Figure 3** Equilibrium paths of post-buckled circular plate for different values of  $\varepsilon_0$  ( $V_s = 10\%$ ).

the initial strain in the SMA fiber. It is clear that an increase in the SMA volume fraction noticeably reduces the post-buckling deformation of the composite plate, and enhances its critical buckling temperature. For a high SMA volume fraction, the thermally buckled plate can revert to its unbuckled configuration in the temperature range of the inverse martensite phase transformation, and the plate will again buckle with further increase in the temperature.

For  $V_s = 10\%$ ,  $20\%$  and various value of  $\varepsilon_0$ , results exhibited in Figures 3 and 4 delineate effects of the thermal load  $\lambda$  on the central deflection  $A$ . These evince that, for a simply supported plate, the initial strain in the SMA fibers has a little influence on the critical buckling temperature but a significant effect on the thermally induced post-buckling deformation because the inverse martensite phase transformation of SMA fibers occurs during the post-buckling region. However, for the clamped plate with  $V_s = 20\%$ , the critical buckling temperature can be enhanced by increasing the pre-strain in the SMA fibers. This is because an increase in  $\varepsilon_0$  increases the temperature at which the inverse martensite phase transformation is completed. It implies that the buckling occurs after the martensite phase

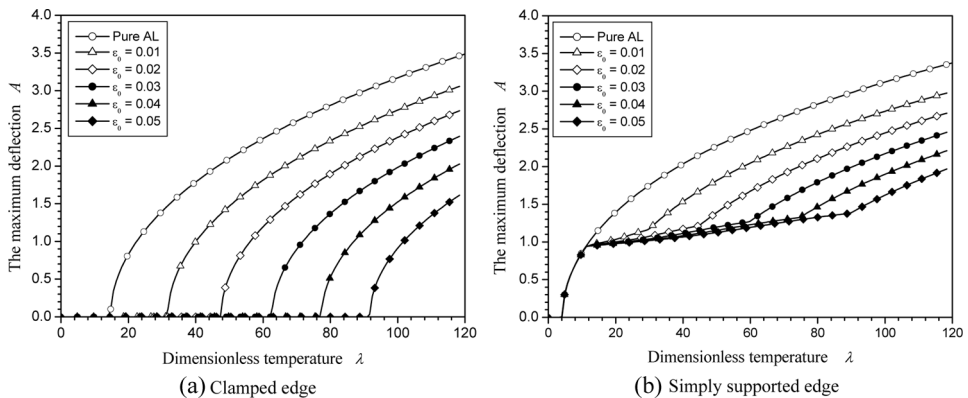


**Figure 4** Equilibrium paths of post-buckled circular plate for different values of  $\varepsilon_0$  ( $V_s = 20\%$ ).

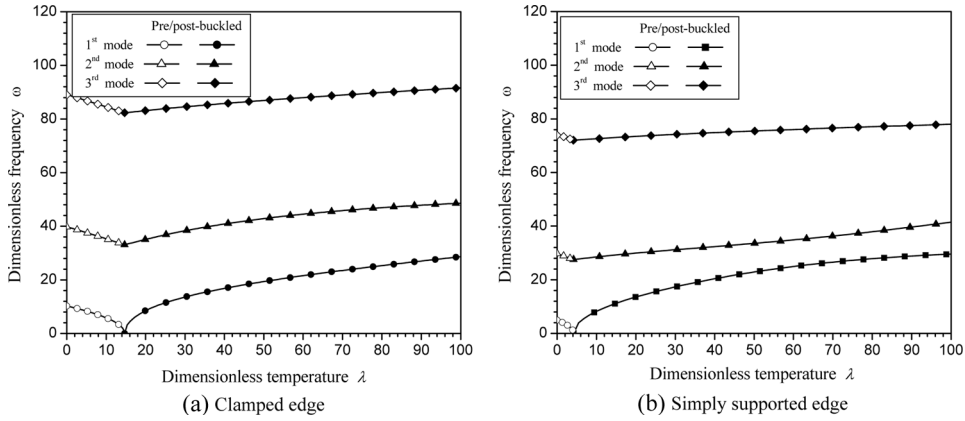


**Figure 5** Dependence of the natural frequencies of the pre/post-buckled plate upon the temperature rise.

has completely been transformed into the austenite phase. Therefore, in general, an increase in either  $\varepsilon_0$  or  $V_s$  will decrease the post-buckling deflection of the plate due to the higher recovery stress in the SMA fibers. These results are qualitatively similar to those for rectangular plates obtained by Zhong [17, 18], Lee [21] and Park [19, 20].

**Vibration**

By simultaneously solving boundary-value problems defined by Eqs. (18)–(21) and (27)–(30), frequencies and the corresponding mode shapes of a thermally pre-buckled and post-buckled SMA fiber reinforced circular plate with the boundary either simply supported or clamped are obtained. Figures 4–7 exhibit the dependence of the first three natural frequencies upon the thermal load parameter

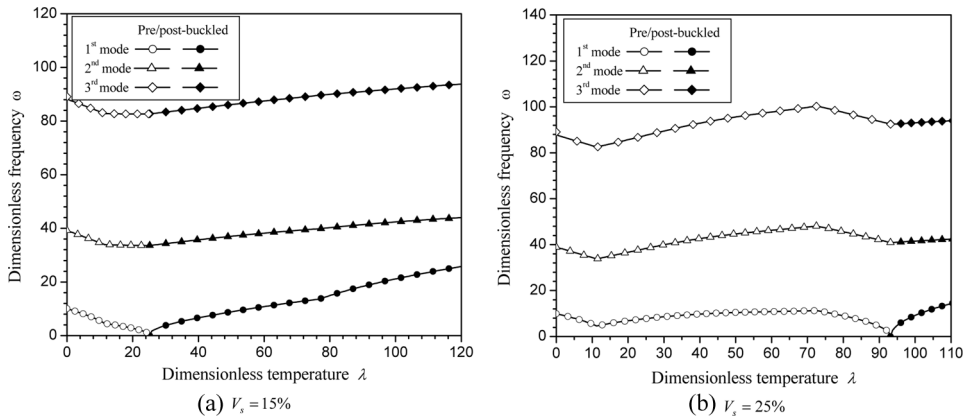


**Figure 6** For  $\varepsilon_0 = 0.04$ , dependence of the natural frequencies of the pre/post-buckled clamped circular plate upon the temperature rise.

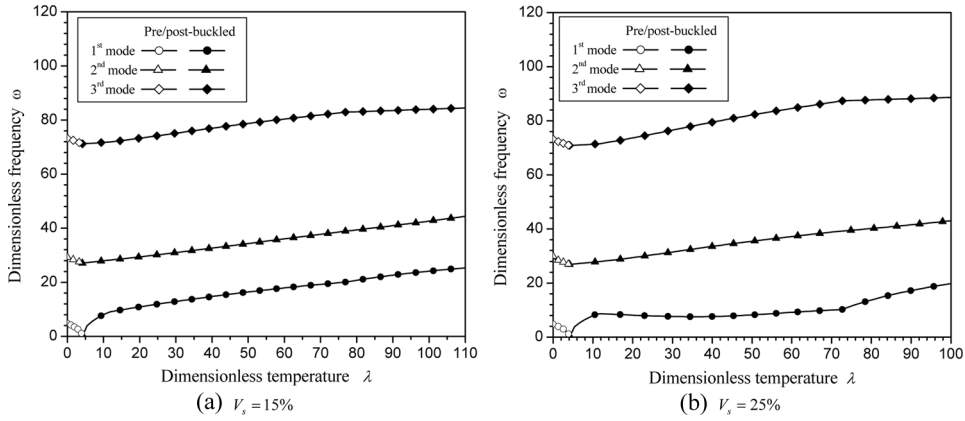


**Figure 7** For  $\varepsilon_0 = 0.04$ , dependence of the natural frequencies of the pre/post-buckled simply supported circular plate upon the temperature rise.

$\lambda$  with and without the SMA fibers in the pre-buckling and the post-buckling regions. From the results shown in Figure 5, we conclude that the first three lowest frequencies of a pre-buckled plate without SMA fibers decrease monotonically with an increase in the temperature, and, as expected, the fundamental frequency approaches zero at the critical temperature. In the post-buckling region, the frequency of the plate increases with an increase in the temperature because the large deflection of the post-buckled plate increases the bending stiffness of the plate [10, 19, 20].

However, for the clamped plate reinforced with the SMA fibers, frequencies decrease first, then increase or adjust, and then decrease in the pre-buckling region for  $V_s = 25\%$  as presented in Figure 6. This phenomenon results from the increase of the bending stiffness due to the recovery stress of SMA with

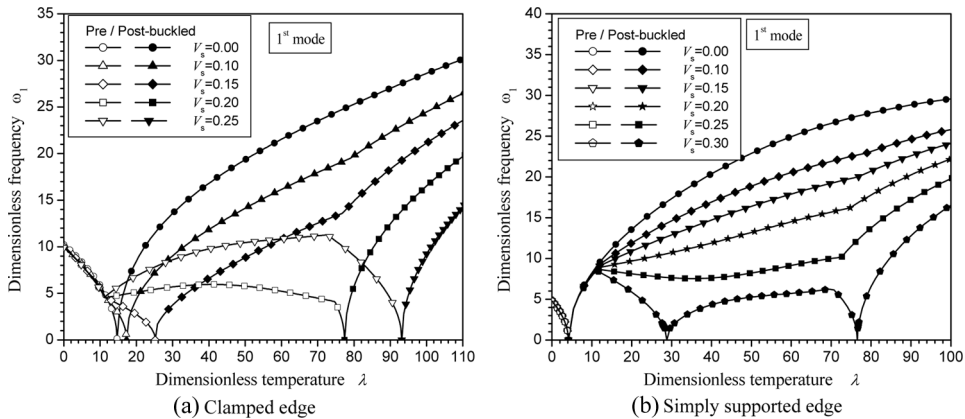


**Figure 8** For  $\varepsilon_0 = 0.04$  and different values of  $V_s$ , fundamental frequencies versus the temperature rise for the circular plate.

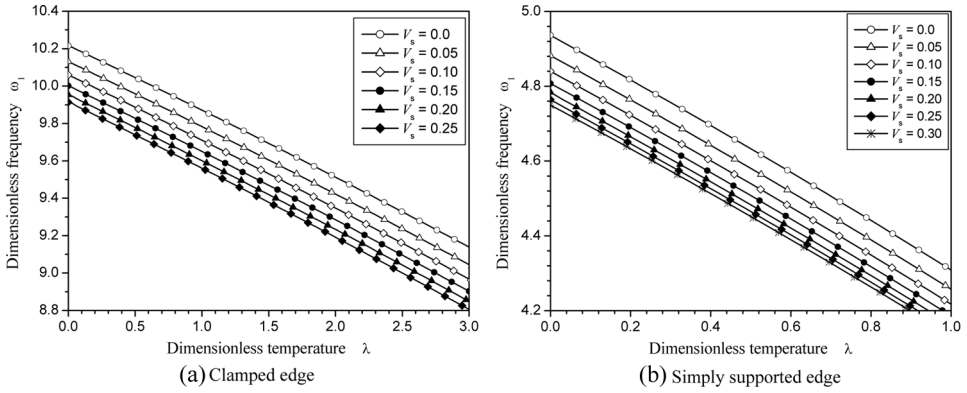


**Figure 9** For  $\epsilon_0 = 0.04$  and different values of  $V_s$ , an expanded view of the fundamental frequencies versus the temperature rise for the circular plate presented in Figure 8.

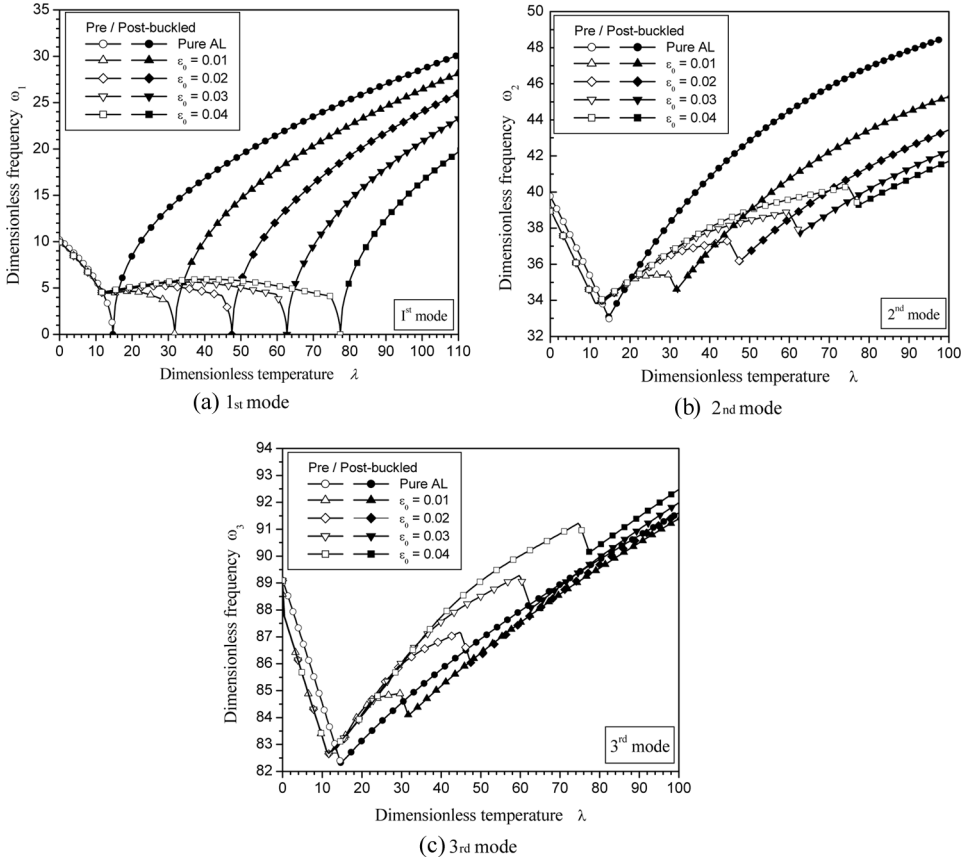


**Figure 10** For  $V_s = 20\%$  and different values of  $\epsilon_0$ , the dependence of the first three lowest frequencies upon the non-dimensional temperature rise for the clamped circular plate.

initial strain [17–20]. In addition, as seen from Figure 6, the temperature range of pre-buckling deformations can be enlarged because of the temperature activation of the embedded SMA fibers. For relatively small volume fractions of SMA fibers, frequencies change in both the pre-buckling and the post-buckling regions, but for relatively large volume fractions of SMA fibers, frequencies adjust only in the pre-buckling region. Frequencies of the simply supported SMA-reinforced plate only decrease in the pre-buckling region as presented in Figure 7. This is because the start temperature of the inverse martensite transformation is larger than the critical buckling temperature for the simply supported plate; thus frequencies adjustment including the control of buckling as discussed in the previous section can only be seen in the post-buckling regime.

Figure 8 displays variation of the fundamental frequency of the clamped and the simply supported plates in the pre- and the post-buckled regions for specified values of  $V_s$ . It is evident that with an increase in  $V_s$  the fundamental frequency is reduced in the post-buckling region because the increased recovery force depresses the post-buckling deflection (Cf. Fig. 2). In Figure 9 we have plotted an enlarged

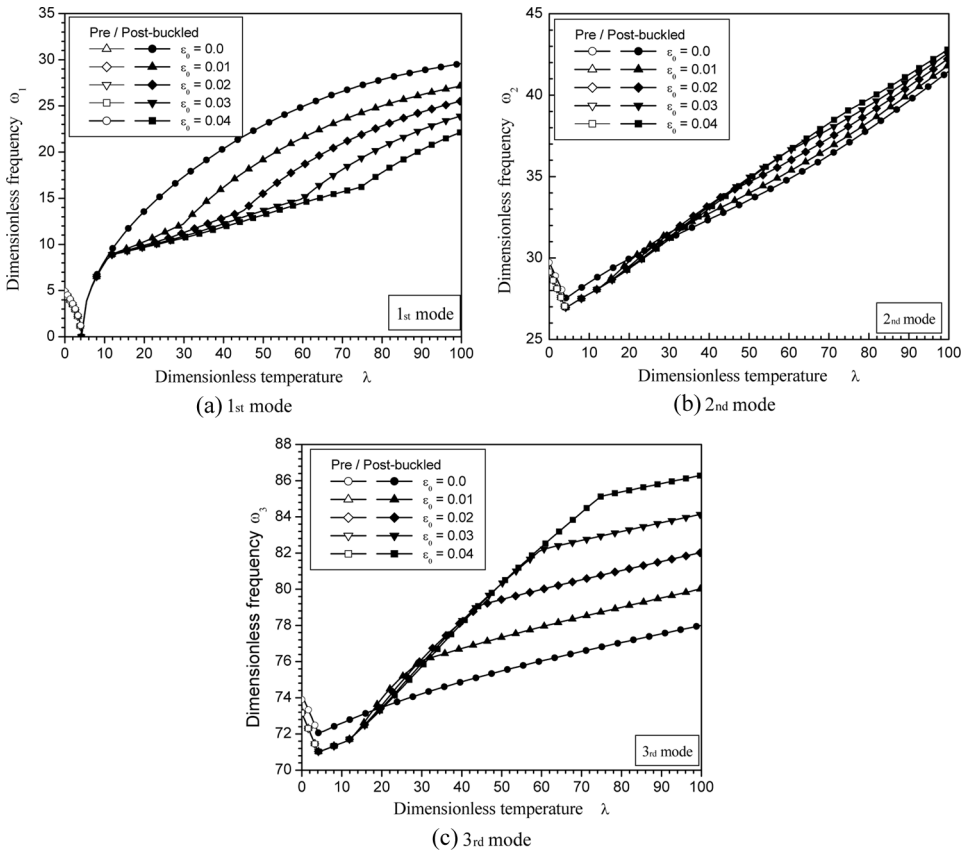


**Figure 11** For  $V_s = 20\%$  and different values of  $\epsilon_0$ , the dependence of the first three lowest frequencies upon the non-dimensional temperature rise for the simply supported circular plate.

view of the local part of the frequency-temperature curves in the pre-buckling region shown in Figure 8. It is clear that the frequency decreases with an increase in the value of  $V_s$ , which primarily is due to the increase of the plate weight and the nonexistence of the recovery stress in SMA fibers as noted by Park et al. [19]. For  $V_s = 20\%$ , we have exhibited in Figures 10 and 11 the influence of the pre-strain in the SMA fibers on the first three lowest frequencies. From Figure 10 we see that the adjustment for the frequency of clamped plate can be realized in the pre-buckling region because the start temperature of inverse martensite transformation is less than the critical buckling temperature. Along with the increase in values of the pre-strain of SMA the pre-buckling region is extended. Nevertheless, as mentioned, SMA fibers embedded in the simply supported plate are activated in the post-buckling region. The variation of frequencies of the plate with an increase in the SMA volume fraction, as shown in Figure 11, is quite interesting.

## CONCLUSIONS

Free vibrations of circular plates reinforced with SMA (NiTiNol) fibers in the radial direction and the plate heated uniformly have been numerically analyzed with the shooting method when the plate has or has not buckled and the plate boundary is either simply supported or clamped. Effects of the volume fraction and the pre-strain in the SMA fibers on the thermal post-buckling deflection and the natural frequencies have been delineated. For a simply supported plate points on the boundary are restrained from moving radially. It is found that the embedding of SMA fibers in a circular plate increases the critical buckling temperature and decreases the post-buckling deflection. However, it has a minimal effect on the critical buckling load but decreases the post-buckling deflection of the simply supported circular plate. This is because the start temperature of inverse martensite phase transformation of the NiTiNol is less than the critical buckling temperature of the plate. The recovery force produced by the pre-strained SMA fibers when stimulated by heating significantly increases the critical buckling temperature for a clamped circular plate, and the recovery force is enhanced by increasing values of both the initial strain and the volume fraction of SMA fibers.

For several values of the pre-strain and the volume fraction of SMA fibers, the three lowest natural frequencies of SMA fiber-reinforced circular plate both in the pre-buckling and the post-buckling regions have been computed. The frequencies increase in the pre-buckling region for the clamped plates and decrease it in the post-buckling region for the simply supported plate. This is due to the increase in the weight of the plate and the decrease in the deflection caused by the SMA fibers [19, 20]. Thus the thermal buckling and the vibration response can be efficiently controlled by adjusting values of the volume fraction of SMA, the pre-strain in the SMA fibers and the temperature rise.

## APPENDIX A

Adopting the mechanics of materials approach, material parameters for the composite are assumed to be related to those of its constituents by the following relations [17–20]:

$$E_r = E_m V_m + E_s V_s = E_m (1 - V_s) + E_s V_s \quad (\text{A-1})$$

$$E_\theta = \frac{E_m E_s}{E_m V_s + E_s V_m} = \frac{E_m E_s}{E_m V_s + E_s (1 - V_s)} \quad (\text{A-2})$$

$$\mu_{r\theta} = \mu_m V_m + \mu_s V_s = \mu_m (1 - V_s) + \mu_s V_s \quad (\text{A-3})$$

$$\mu_{r\theta} = \mu_{\theta r} k_0, \quad k = E_\theta / E_r \quad (\text{A-4})$$

$$\alpha_r = \frac{E_m \alpha_m V_m + E_s \alpha_s V_s}{E_r} = \frac{E_m \alpha_m (1 - V_s) + E_s \alpha_s V_s}{E_r} \quad (\text{A-5})$$

$$\alpha_\theta = \alpha_m V_m + \alpha_s V_s = \alpha_m (1 - V_s) + \alpha_s V_s \quad (\text{A-6})$$

$$\rho = \rho_m V_m + \rho_s V_s = \rho_m (1 - V_s) + \rho_s V_s \quad (\text{A-7})$$

where subscripts ‘*m*’ and ‘*s*’ indicate quantities for the matrix and the SMA fiber, respectively.

## REFERENCES

1. T. R. Tauchert, Thermally Induced Flexure, Buckling and Vibration of Plates, *Applied Mechanics Review*, vol. 44, pp. 347–360, 1991.
2. E. A. Thornton, Thermal Buckling of Plates and Shells, *Applied Mechanics Review*, vol. 46, pp. 485–506, 1993.
3. L. Librescu, W. Lin, M. P. Nemeth, and J. H. Starnes, Jr., Vibration of Geometrically Imperfect Panels Subjected to Thermal and Mechanical Loads, *J. Spacecraft Rockets*, vol. 33, pp. 285–291, 1996.
4. L. Librescu and W. Lin, Vibration of Thermomechanically Loaded Flat and Curved Panel Taking into Account Geometric Imperfections and Tangential Edge Restraints, *Int. J. Solids and Structures*, vol. 34, pp. 2161–2181, 1997.
5. S.-R. Li and Y.-H. Zhou, Shooting Method for Non-Linear Vibration and Thermal Buckling of Heated Orthotropic Circular Plates, *J. Sound and Vibration*, vol. 248, pp. 379–386, 2001.
6. S.-R. Li, Y.-H. Zhou, and X. Song, Non-linear Vibration and Thermal Buckling of an Orthotropic Annular Plate with a Centric Rigid Mass, *J. Sound and Vibration*, vol. 251, pp. 141–152, 2002.
7. D. M. Lee and I. Lee, Vibration Behaviors of Thermally Post-Buckled Anisotropic Plates Using First-Order Shear Deformation Plate Theory, *Computers and Structures*, vol. 63, pp. 371–378, 1997.
8. I. K. Oh, J. H. Han, and I. Lee, Post-Buckling and Vibration Characteristics of Piezolaminated Composite Plate Subjected to Thermo-Piezoelectric Loads, *J. Sound and Vibration*, vol. 233, pp. 19–40, 2000.
9. J. S. Park and J. H. Kim, Thermal Postbuckling and Vibration Analyses of Functionally Graded Plates, *J. Sound and Vibration*, vol. 289, pp. 77–93, 2006.
10. S. R. Li, R. C. Batra, and L. S. Ma, Free Vibration of Orthotropic Circular Plates with Thermal Post-Buckled Deformation, *J. Thermal Stresses*, vol. 30, pp. 43–57, 2007.
11. C. A. Rogers, Active Vibration and Structural Acoustic Control of Shape Memory Alloy Hybrid Composites: Experimental Results, *J. Acoustic Society of America*, vol. 88, pp. 2803–2811, 1990.
12. C. A. Rogers, C. Liang, and C. R. Fuller, Modeling of Shape Memory Alloy Hybrid Composites for Structural Acoustic Control, *J. Acoustic Society of America*, vol. 89, pp. 210–220, 1991.
13. C. A. Rogers, C. Liang, and J. Jia, Structural Modification of Simply Supported Laminated Plates Using Shape Memory Alloy Fibers, *Computers and Structures*, vol. 38, pp. 569–580, 1991.

14. J. Ro and A. Baz, Nitinol-Reinforced Plates: Part I–III, *Composites Engineering*, vol. 5, pp. 61–106, 1999.
15. W. Ostachowicz, M. Krawczuk, and A. Zak, Natural Frequencies of a Multilayer Composite Plate with Shape Memory Alloy Wires, *Finite Element in Analysis and Design*, vol. 32, pp. 71–83, 1999.
16. W. Ostachowicz, M. Krawczuk, and A. Zak, Dynamic and Buckling of a Multilayer Composite Plate with Embedded SMA Wires. *Composite Structures*, vol. 48, pp. 163–167, 2000.
17. Z. W. Zhong, Reduction of Thermal Deflection and Random Response of Composite Structures with Embedded Shape Memory Alloy at Elevated Temperature, *PhD Thesis*, Old Dominion University, Virginia, 1998.
18. Z. W. Zhong, Buckling and Post-Buckling of Shape Memory Alloy Fiber Reinforced Composite Plates, *Buckling and Post-Buckling of Composite Structures*, 41/PVP, vol. 293. ASME, pp. 115–132, 1994.
19. J.-S. Park, J.-H. Kim, and S.-H. Moon, Vibration of Thermally Post-Buckling Composite Plates Embedded with Shape Memory Alloy Fibers, *Composite Structures*, vol. 63, pp. 179–188, 2004.
20. J.-S. Park, J.-H. Kim, and S.-H. Moon, Thermal Post-Buckling and Flutter Characteristics of Composite Plates Embedded with Shape Memory Alloy Fibers, *Composites Part B: Engineering*, vol. 36, pp. 627–636, 2005.
21. H.-J. Lee, J.-J. Lee, and J.-S. Huh, A Simulation Study in the Thermal Buckling Behavior of Laminated Composite Shells with Embedded Shape Memory Alloy Wires, *Composite Structure*, vol. 47, pp. 463–469, 1999.
22. S. P. Thompson and J. Loughlan, Adaptive Post-Buckling Response of Carbon Fiber Composites Plates Employing SMA Actuators, *Composite Structures*, vol. 38, pp. 667–678, 1997.
23. S. P. Thompson and J. Loughlan, The Control of the Post-Buckling Response in Thin Composite Plates Using Smart Technology, *Thin-Walled Structures*, vol. 36, 231–263, 2000.
24. R. X. Zhang et al., Vibration Characteristics of Laminated Composite Plates with Embedded Shape Memory Alloys, *Composite Structures*, vol. 74, pp. 389–398, 2006.
25. L. C. Brinson, One-Dimensional Constitutive Behavior and Shape Memory Alloys: Thermo-Mechanical Derivation with Non-Constant Material Functions and Redefined Martensite Internal Variable, *J. Intelligent Material System and Structures*, vol. 4, pp. 229–243, 1993.
26. L.-S. Ma and T.-J. Wang, Nonlinear Bending and Post-Buckling of a Functionally Graded Circular Plate under Mechanical and Thermal Loadings, *Int. J. Solids and Structures*, vol. 40, pp. 3311–3330, 2003.
27. K. K. Raju and G. V. Rao, Thermal Post-Buckling of Circular Plates, *Computers and Structures*, vol. 18, pp. 1179–1182, 1984.
28. U. S. Gupta and A. H. Ansari, Effect of Elastic Foundation on Asymmetric Vibration of Polar Orthotropic Linearly Tapered Circular Plates, *J. Sound and Vibration*, vol. 254, pp. 411–420, 2000.
29. C. L. Huang and H. S. Wolker, Non-Linear Vibration of Hinged Circular Plate with a Concentric Rigid Mass, *J. Sound and Vibration*, vol. 126, pp. 9–17, 1988.
30. S. Timoshenko and S. Woinowsky-Krieger, *Theory of Plates and Shells*, 2nd Ed., McGraw-Hill, New York, 1959.
31. B. Jiang and R. C. Batra, Micromechanical Modeling of a Composite Containing Piezoelectric and Shape Memory Alloy Inclusions, *J. Intelligent Materials and Systems*, vol. 12, pp. 165–182, 2001.

32. M. Cherkaoui, Q. P. Sun, and G. Q. Song, Micromechanics Modeling of Composites with Ductile Matrix and Shape Memory Alloy Reinforcement, *Int. J. Solids and Structures*, vol. 37, pp. 1577–1594, 2000.
33. D. C. Lagoudas, J. G. Boyd, and Z. Bo, Micromechanics of Active Composites with SMA Fibers, *ASME J. Engineering Materials and Technology*, vol. 116, pp. 337–347, 1994.
34. Z. K. Lu and G. J. Weng, A Two-Level Micromechanical Theory for a Shape Memory Alloy Reinforced Composite, *Int. J. Plasticity*, vol. 16, pp. 1289–1307, 2000.
35. K. Tanaka, S. Kobayashi, and Y. Sato, Thermomechanics of Transformation Pseudoelasticity and Shape Memory Effect in Alloys, *Int. J. Plasticity*, vol. 2, pp. 59–72, 1986.